Joint Bayesian Deconvolution And Point Spread Function Estimation For Ultrasound Imaging

Ningning Zhao, Adrian Basarab, Denis Kouamé, Jean-Yves Tourneret

JOINT BAYESIAN DECONVOLUTION AND POINT SPREAD FUNCTION ESTIMATION FOR ULTRASOUND IMAGING

Ningning Zhao[1,2]*, Adrian Basarab* [2]*, Denis Kouame*[2]*, Jean-Yves Tourneret*[1,3]

[1] University of Toulouse, INP/ENSEEIHT-IRIT, 2 rue Charles Camichel, BP 7122, 31071 Toulouse Cedex 7, France

[2] University of Toulouse, IRIT, CNRS UMR 5505, Université Paul Sabatier, Toulouse, France

[3] TéSA Laboratory, 14-16 Port Saint-Etienne, 31000 Toulouse, France

{nzhao, jean-yves.tourneret}@enseeiht.fr, {adrian.basarab, denis.kouame}@irit.fr

ABSTRACT

This paper addresses the problem of blind deconvolution for ultrasound images within a Bayesian framework. The prior of the unknown ultrasound image to be estimated is assumed to be a product of generalized Gaussian distributions. The point spread function of the system is also assumed to be unknown and is assigned a Gaussian prior distribution. These priors are combined with the likelihood function to build the joint posterior distribution of the image and PSF. However, it is difficult to derive closed-form expressions of the Bayesian estimators associated with this posterior. Thus, this paper proposes to build estimators of the unknown model parameters from samples generated according to the model posterior using a hybrid Gibbs sampler. Simulation results performed on synthetic data allow the performance of the proposed algorithm to be appreciated.

Index Terms— Ultrasound imaging, image deconvolution, Bayesian inference, Gibbs sampler.

1. INTRODUCTION

Ultrasound (US) imaging is widely used due to its advantages such as being portable, cost effective and noninvasive. However, the US images are contaminated by an intrinsic noise called speckle and have low contrast and relatively low spatial resolution at a given frequency. A 2D convolution model between the tissue reflectivity image and the system point spread function (PSF) is commonly used to model US images. As a consequence, deconvolution methods are widely used to improve the quality of US images.

Deconvolution is an ill-posed problem. In US imaging, Gaussian and Laplacian distributions are widely used as *a priori* knowledge for the reflectivity image to solve this ill-posed problem [1, 2]. Moreover, the generalized Gaussian distribution (GGD) has been recently shown to be appropriate for the statistical properties of US images [3]. Based on this assumption, Alessandrini *et al.* have developed an EM-based US deconvolution algorithm with GGD prior that we have recently improved using a hierarchical Bayesian model [4]. An important challenge in US image deconvolution is that the PSF is unknown in practical situations. Most of the reported methods consider the estimation of the PSF as an initialization step, followed by an US image deconvolution [5], [6]. Methods for estimating jointly the unknown US image and the PSF have also been recently proposed, see e.g., [1] which proposed Gaussian priors for both tissue reflectivity and PSF.

Unfortunately, the PSF is shift-variant along the axial direction in US imaging. This problem has been handled by partitioning the image into several regions in which the PSF is assumed shift-invariant locally [5]. Using this assumption, we propose to solve the blind deconvolution problem in a Bayesian framework. Precisely, GGD priors are assigned to the US reflectivities and coupled with a Gaussian prior for the PSF. A new posterior distribution is then obtained for joint image deconvolution and PSF estimation. However, it is difficult to compute closed-form expressions of the Bayesian estimators for the unknown parameters of this posterior. Consequently, we study an MCMC sampling method generating samples according to the posterior of our model which are further used to construct Bayesian estimators. The reported simulations show that the proposed method outperforms our previous approach using an estimated PSF resulting from a pre-processing step [4].

The paper is organized as follows. Section 2 introduces the proposed Bayesian model and the associated hybrid Gibbs sampler for the deconvolution of ultrasound images with an inaccurate knowledge about the point spread function. Simulation results are presented in Section 3 and conclusions are reported in Section 4.

2. BAYESIAN FRAMEWORK

2.1. Problem Statement

The linear model used for US image restoration can be defined using the following matrix-vector formulation

$$\mathbf{y} = \mathbf{H}\mathbf{x} + \mathbf{n} \tag{1}$$

where $\mathbf{y}$ and $\mathbf{x}$ are vectors of $\mathbb{R}^{N\times 1}$ obtained after lexicographical order of the radio-frequency (RF) and tissue reflectiviy images, $\mathbf{n}$ is an additive white Gaussian noise (AWGN) and $\mathbf{H} \in \mathbb{R}^{N\times N}$ is a circulant matrix associated with the PSF. Note that an efficient implementation of the matrix-vector product in (1) is obtained by using the direct and inverse Fourier transforms as follows

$$\mathbf{H}\mathbf{x} = \mathbf{F}^T[\mathbf{F}\mathbf{h}. * \mathbf{F}\mathbf{x}] = \mathbf{F}^T[\tilde{\mathbf{h}}. * \tilde{\mathbf{x}}] \tag{2}$$

where the matrices $\mathbf{F}$ and $\mathbf{F}^T$ correspond to Fourier and inverse Fourier transforms, $.*$ is the Hadamard product, $\mathbf{h}$ is the first row of $\mathbf{H}$ and $\tilde{\boldsymbol{\phi}} = \mathbf{F}\boldsymbol{\phi}$ is the Fourier transform of the vector $\boldsymbol{\phi}$. The relation (2) is based on the property of circulant matrices, i.e., $\mathbf{H} = \mathbf{F}^T\boldsymbol{\Sigma}_{\boldsymbol{H}}\mathbf{F}$, where $\boldsymbol{\Sigma}_{\boldsymbol{H}} = \text{diag}(\tilde{\mathbf{h}})$. The goal of the blind deconvolution problem studied here is to estimate the reflectivity image $\mathbf{x}$ and the PSF $\mathbf{H}$ by using a hierarchical Bayesian model.

2.2. Hierarchical Bayesian model

The hierarchical Bayesian model proposed in this work requires to define appropriated prior distributions for the unknown vector $\boldsymbol{\Theta} =$

$(\mathbf{x}, \mathbf{H}, \sigma_n^2)$. The joint posterior distribution of $\boldsymbol{\Theta}$ can then be calculated from the product of the likelihood function and the prior distributions. The likelihood function and the prior distributions considered in this paper are defined in the following sections. Consequently, the Bayesian estimators MAP or MMSE can be adapted for the estimation of the unknown variable. In this paper, the MMSE estimator is employed.

2.2.1. Likelihood

Assuming an AWGN sequence with covariance matrix $\sigma_n^2 \mathbf{I}_{N\times N}$, the likelihood function associated with model (1) is

$$p(\mathbf{y}|\boldsymbol{\Theta}) = \frac{1}{(2\pi\sigma_n^2)^{N/2}} \exp\left(-\frac{1}{2\sigma_n^2}\|\mathbf{y} - \mathbf{H}\mathbf{x}\|_2^2\right) \tag{3}$$

where $\|\cdot\|_2$ is the usual ℓ_2-norm.

2.2.2. Priors

A. Reflectivity image. We assume that the pixels of the US image are independent random variables distributed according to generalized Gaussian distributions (GGDs) [3]. Moreover, the pixels of the US image belonging to different homogeneous regions are supposed to be distributed according to GGDs with different parameters. This assumption makes sense in applications such as tumor detection, where the tumor and the image background are characterized by different sets of parameters. Precisely, we introduce a label vector $\mathbf{z} \in \mathbb{R}^{N\times 1}$ to map the image into the different homogeneous regions. The ith label is such that $z_i = k$ if and only if the corresponding pixel x_i belongs to the class $k \in \{1, ..., K\}$. The conditional distribution of the pixel x_i is defined as

$$x_i|z_i = k \sim \mathcal{GGD}(\xi_k, \gamma_k)$$

where ξ_k and γ_k are the shape and scale parameters of the kth class. Conditioned on the label vector, we obtain the following prior for the reflectivity image

$$p(\mathbf{x}|\mathbf{z}, \boldsymbol{\xi}, \boldsymbol{\gamma}) = \prod_{k=1}^{K} \frac{1}{\left[2\gamma_k^{1/\xi_k}\Gamma(1+1/\xi_k)\right]^{N_k}} \exp\left(-\frac{\|\mathbf{x}_k\|_{\xi_k}^{\xi_k}}{\gamma_k}\right) \tag{4}$$

where $\|\mathbf{x}_k\|_\xi = (\sum_{i=1}^{N_k} |x_i|^\xi)^{1/\xi}$ denotes the ℓ_ξ-norm, $\mathbf{x}_k$ contains all the pixels assigned to class k, the shape and scale parameter vectors are denoted as $\boldsymbol{\xi} = (\xi_1, ..., \xi_K)$ and $\boldsymbol{\gamma} = (\gamma_1, ..., \gamma_K)$ with $\gamma_k = \left[\sqrt{\sigma_k^2\Gamma(1/\xi_k)/\Gamma(3/\xi_k)}\right]^{\xi_k}$ (σ_k^2 is the variance of class k), N_k is the number of pixels in class k and $\Gamma(\cdot)$ is the gamma function. In this paper, the labels $\mathbf{z}$ are assumed to be known. However, it could be interesting to estimate them with a Markov random field prior as in [4].

B. Point Spread Function. The circular matrix $\mathbf{H}$ can be obtained by cyclic shift of its first row $\mathbf{h}$. Keeping in mind that the convolution model is expressed in the Fourier domain (see (2)), a multivariate Gaussian distribution is chosen for the prior of $\tilde{\mathbf{h}}$ [7]

$$p(\tilde{\mathbf{h}}) = \frac{1}{(2\pi\sigma_h^2)^{N/2}} \exp\left(-\frac{1}{2\sigma_h^2}\|\tilde{\mathbf{h}} - \tilde{\mathbf{h}}_0\|_2^2\right) \tag{5}$$

where $\tilde{\mathbf{h}}_0$ is the Fourier transform of the first row of the circulant matrix $\mathbf{H}_0$ and $\mathbf{H}_0$ is an initial estimation of the PSF (for instance obtained with the method of [6]).

C. Noise variance In the presence of AWGN, it is typical to assign a conjugate inverse gamma prior to the noise variance, i.e.,

$$p(\sigma_n^2) = \frac{\nu^\alpha}{\Gamma(\alpha)} \frac{1}{(\sigma_n^2)^{\alpha+1}} \exp\left(-\frac{\nu}{\sigma_n^2}\right) \mathbf{1}_{\mathbb{R}^+}(\sigma_n^2) \tag{6}$$

where $\mathbf{1}_A(.)$ is the indicator function on the set A. The two adjustable parameters α, ν make this prior very flexible and appropriate for many applications.

2.2.3. Hyperpriors

The priors introduced above depend on some hyperparameters that need to be fixed *a priori* or estimated within the algorithm. This paper assumes that the hyperparameters associated with the noise variance (α, ν), the PSF (σ_h^2) and the reflectivity image $(\mathbf{z})$ are fixed *a priori*. However, the hyperparameters of the reflectivity image $\boldsymbol{\xi}, \boldsymbol{\gamma}$ are estimated via a hierarchical Bayesian model. We denote the hyperparameter vector to be estimated as $\boldsymbol{\Phi} = \{\boldsymbol{\xi}, \boldsymbol{\gamma}\}$. The hyperprior of $\boldsymbol{\Phi}$ is defined as $p(\boldsymbol{\Phi}) = p(\boldsymbol{\xi})p(\boldsymbol{\gamma})$ with

$$p(\boldsymbol{\xi}) = \prod_{k=1}^{K} p(\xi_k) = \prod_{k=1}^{K} \frac{1}{3}\mathbf{1}_{[0,3]}(\xi_k) \tag{7}$$

$$p(\boldsymbol{\gamma}) = \prod_{k=1}^{K} p(\gamma_k) = \prod_{k=1}^{K} \frac{1}{\gamma_k}\mathbf{1}_{\mathbb{R}+}(\gamma_k). \tag{8}$$

We should notice that the choices above cover all the possible values of the shape and scale parameters that one may encounter in practical situations [4], [8].

2.2.4. Joint posterior function

Using Bayes' rule, the joint posterior distribution of our model is proportional to the product of the likelihood and the priors. Precisely, the following result can be obtained

$$\begin{aligned} p(\boldsymbol{\Theta}, \boldsymbol{\Phi}|\mathbf{y}) &\propto p(\mathbf{y}|\boldsymbol{\Theta}, \boldsymbol{\Phi})p(\boldsymbol{\Theta}, \boldsymbol{\Phi}) \\ &\propto p(\mathbf{y}|\mathbf{x}, \mathbf{H}, \sigma_n^2, \boldsymbol{\xi}, \boldsymbol{\gamma})p(\mathbf{x}, \mathbf{H}, \sigma_n^2, \boldsymbol{\xi}, \boldsymbol{\gamma}) \\ &\propto p(\mathbf{y}|\mathbf{x}, \mathbf{H}, \sigma_n^2)p(\mathbf{x}|\boldsymbol{\xi}, \boldsymbol{\gamma})p(\mathbf{H})p(\sigma_n^2) \end{aligned} \tag{9}$$

where the different probability density functions (pdfs) have been defined in (3), (4), (5) and (6). Closed-form expressions of the Bayesian estimators associated with the posterior (9) are clearly difficult to obtain. In such situation, one can use simulation methods which generate samples distributed according to the posterior of interest and use these samples to compute the estimators of the unknown model parameters. It is the objective of the next section.

2.3. Hybrid Gibbs Sampler

The Gibbs sampler is one of the most popular Markov chain Monte Carlo (MCMC) methods. It generates samples from a Markov chain whose target distribution is the posterior distribution of interest. Each step of the sampler consists of generating according to the conditional distributions associated with the target distribution. This section discusses how to sample according to the conditional distributions of (9).

2.3.1. Noise variance

The conditional distribution of the noise variance σ_n^2 is

$$p(\sigma_n^2|\mathbf{y},\mathbf{x},\boldsymbol{\xi},\boldsymbol{\gamma},\mathbf{H}) \propto p(\mathbf{y}|\mathbf{x},\sigma_n^2,\boldsymbol{\xi},\boldsymbol{\gamma},\mathbf{H})p(\sigma_n^2) \propto \frac{1}{(\sigma_n^2)^{\frac{N}{2}+\alpha+1}} \exp\left(-\frac{1}{2\sigma_n^2}\|\mathbf{y}-\mathbf{H}\mathbf{x}\|_2^2 - \frac{\nu}{\sigma_n^2}\right).$$

It is the inverse gamma distribution

$$\mathcal{IG}\left(\alpha+\frac{N}{2}, \nu+\frac{1}{2}\|\mathbf{y}-\mathbf{H}\mathbf{x}\|_2^2\right) \tag{10}$$

which is straightforward to sample.

2.3.2. Reflectivity image $\mathbf{x}$

The conditional distribution of the US reflectivity image is

$$p(\mathbf{x}|\mathbf{y},\sigma_n^2,\mathbf{H},\boldsymbol{\Phi}) \propto p(\mathbf{y}|\mathbf{x},\sigma_n^2,\mathbf{H},\boldsymbol{\Phi})p(\mathbf{x}|\boldsymbol{\Phi}) \propto \exp\left(-\frac{1}{2\sigma_n^2}\|\mathbf{y}-\mathbf{H}\mathbf{x}\|_2^2 - \sum_{k=1}^{K}\frac{\|\mathbf{x}_k\|_{\xi^k}^{\xi^k}}{\gamma^k}\right). \tag{11}$$

Generating samples from (11) is complicated due to the high dimensionality of the image $\mathbf{x}$ and to the non-quadratic term $\|\mathbf{x}_k\|_{\xi^k}^{\xi^k}$. In this work, we propose to use a Hamiltonian Monte Carlo (HMC) method for this generation. This method has shown interesting results in the case of a known PSF (see [4] for details).

2.3.3. Point Spread Function

In this paper, we propose to sample $\tilde{\mathbf{h}}$ instead of $\mathbf{H}$. The likelihood function can be rewritten as follows

$$p(\mathbf{y}|\mathbf{x},\sigma_n^2,\boldsymbol{\Phi},\tilde{\mathbf{h}}) = \frac{1}{(2\pi\sigma_n^2)^{N/2}}\exp\left(-\frac{1}{2\sigma_n^2}\|\tilde{\mathbf{y}}-\boldsymbol{\Sigma}_{\boldsymbol{H}}\tilde{\mathbf{x}}\|_2^2\right) = \frac{1}{(2\pi\sigma_n^2)^{N/2}}\exp\left(-\frac{1}{2\sigma_n^2}\|\tilde{\mathbf{y}}-\boldsymbol{\Sigma}_{\boldsymbol{X}}\tilde{\mathbf{h}}\|_2^2\right) \tag{12}$$

where $\boldsymbol{\Sigma}_{\boldsymbol{H}} = \text{diag}(\tilde{\mathbf{h}})$ and $\boldsymbol{\Sigma}_{\boldsymbol{X}} = \text{diag}(\tilde{\mathbf{x}})$. Combining with the prior of $\tilde{\mathbf{h}}$, the conditional distribution of $\tilde{\mathbf{h}}$ is defined as

$$p(\tilde{\mathbf{h}}|\mathbf{y},\mathbf{x},\sigma_n^2,\boldsymbol{\Phi}) \propto p(\mathbf{y}|\mathbf{x},\sigma_n^2,\boldsymbol{\Phi},\tilde{\mathbf{h}})p(\tilde{\mathbf{h}}) \propto \exp\left(-\frac{1}{2\sigma_n^2}\|\tilde{\mathbf{y}}-\boldsymbol{\Sigma}_{\boldsymbol{X}}\tilde{\mathbf{h}}\|_2^2\right)\exp\left(-\frac{1}{2\sigma_h^2}\|\tilde{\mathbf{h}}-\tilde{\mathbf{h}}_0\|_2^2\right). \tag{13}$$

The conditional distribution (13) is a multivariate Gaussian distribution

$$\mathcal{N}(\tilde{\mathbf{m}}_{\text{post}}, \tilde{\mathbf{R}}_{\text{post}}) \tag{14}$$

with

$$\tilde{\mathbf{R}}_{\text{post}}^{-1} = \frac{\mathbf{I}}{\sigma_h^2} + \frac{|\boldsymbol{\Sigma}_{\boldsymbol{X}}|^2}{\sigma_n^2},\ \tilde{\mathbf{m}}_{\text{post}} = \tilde{\mathbf{R}}_{\text{post}}\left(\frac{\tilde{\mathbf{h}}_0}{\sigma_h^2} + \frac{\boldsymbol{\Sigma}_{\boldsymbol{X}}{}^T\tilde{\mathbf{y}}}{\sigma_n^2}\right) \tag{15}$$

where the subscript "post" stands for "posterior". Note that (14) is easy to sample and that the circulant matrix $\mathbf{H}$ can be easily obtained from $\tilde{\mathbf{h}}$ by inverse Fourier transform and cyclic shift.

2.3.4. Hyperparameters

A. Shape parameter $\boldsymbol{\xi}$ Assuming a priori independence between the different shape parameters, the conditional distribution of parameter ξ_k can be obtained as follows

$$p(\xi_k|\boldsymbol{\Theta},\boldsymbol{\gamma},\boldsymbol{\xi}_{-k}) \propto p(\mathbf{y}|\mathbf{x},\sigma_n^2,\mathbf{H},\boldsymbol{\xi},\boldsymbol{\gamma})p(\mathbf{x}_k|\xi_k,\gamma_k)p(\xi_k) \propto a_k^{N_k}\exp\left(-\frac{\|\mathbf{x}_k\|_{\xi_k}^{\xi_k}}{\gamma_k}\right)\mathbf{1}_{[0,3]}(\xi_k) \tag{16}$$

where $\boldsymbol{\xi}_{-k} = (\xi_1,...,\xi_{k-1},\xi_{k+1},...,\xi_K)$ for $k \in \{1,...,K\}$ and where $\mathbf{x}_k$ contains all the pixels assigned to the kth class.

The conditional distribution (16) is not easy to sample directly. Thus, we propose to consider random walk Metropolis Hastings (MH) moves with appropriate proposals [9]. More specifically, a Gaussian distribution whose variance is adjusted *a priori* in order to obtain a suitable acceptance ratio has been employed in our algorithm. The candidates generated using this proposal are then accepted/rejected according to the standard MH acceptance ratio.

B. Scale parameter $\boldsymbol{\gamma}$ Assuming the different scale parameters are a priori independent, the conditional distributions of the scale parameters of the proposed GGDs can be written

$$p(\gamma_k|\boldsymbol{\Theta},\boldsymbol{\xi},\boldsymbol{\gamma}_{-k}) \propto p(\mathbf{y}|\mathbf{x},\sigma_n^2,\mathbf{H},\boldsymbol{\xi},\boldsymbol{\gamma})p(\mathbf{x}_k|\xi_k,\gamma_k)p(\gamma_k) \propto \mathcal{IG}\left(\frac{N_k}{\xi_k}, \|\mathbf{x}_k\|_{\xi_k}^{\xi_k}\right) \tag{17}$$

where $\boldsymbol{\gamma}_{-k} = (\gamma_1,...,\gamma_{k-1},\gamma_{k+1},...,\gamma_K)$ for $k \in \{1,...,K\}$. Drawing samples from the inverse gamma distribution (17) is straightforward.

2.3.5. Final Algorithm

The hybrid Gibbs sampler resulting from the previous sections is summarized in Alg. 8. After removing the burn-in period of the sampler, the remaining samples are averaged to compute the MMSE estimates of the different unknown parameters.

Algorithm 1: Hybrid Gibbs Sampler

```
   /* Initialization                                   */
1  /* Sampling procedure                               */
2  for i = 1 : N_mc do
3      Sampling σ_n^2 according to (10).
4      Sampling x according to (11) with a HMC method.
5      Sampling h̃ according to (14).
6      Sampling ξ according to (16) using a Metropolis
       Hastings move with a Gaussian proposal.
7      Sampling γ according to (17).
8  end
```

3. SIMULATION RESULTS

In this section, we present results obtained with synthetic US images to validate the performance of the proposed algorithm. The US image simulation follows the approach described in [2]. Specifically, the RF image is obtained by 2D convolution of a reflectivity image (of size 50×50) shown in Fig. 1(a) and a known PSF (of size 11×11) simulated by Field II (developed by Jensen *et. al.*), highlighted in Fig. 2(a). The samples of $\mathbf{x}$ are independent

and identically distributed according to GGDs with different parameters inside and outside the disk located in the center of the image ($\mathcal{GGD}(\xi_{\text{in}} = 1.8, \gamma_{\text{in}} = 50)$ and $\mathcal{GGD}(\xi_{\text{out}} = 0.6, \gamma_{\text{out}} = 0.4)$). Moreover the RF image is contaminated by an AWGN corresponding to a blurred-signal-to-noise-ratio (BSNR)[1] of $40dB$.

Fig. 1 shows the images estimated by the proposed method and the method of [4]. Note that the method of [4] requires to estimate the PSF in a preprocessing step using the algorithm of [6] and that it was shown to provide better deconvolution results than the EM algorithm of [3]. The objective of this simulation is to evaluate whether the performance of the joint estimation of the image and PSF can be improved or not when compared to the case where the PSF is estimated in a preprocessing step. Visually, one can observe that the reflectivity image estimated with our method is very similar to the true one, both in native and B-mode representations. The B-mode is a commonly used representation of US images based on envelope detection and log-compression. Quantitative results reported in Table 1 show (in terms of ISNR, NRMSE and PSNR) that we obtain a better performance with the proposed method when compared to [4]. Note that the higher the values of ISNR, PSNR, the better the performance. Conversely, the lower the NRMSE, the better.

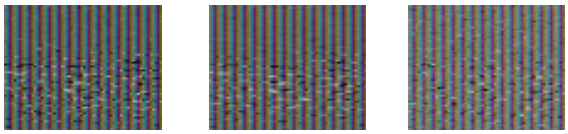

(a) true $\mathbf{x}$ (b) $\hat{\mathbf{x}}$(proposed) (c) $\hat{\mathbf{x}}$ ([4])

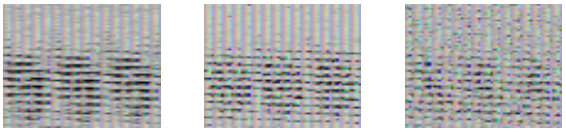

(d)Bmode of (a) (e)Bmode of (b) (f)Bmode of (c)

Fig. 1. Original and restored US images (top: RF images, bottom: B-mode images).

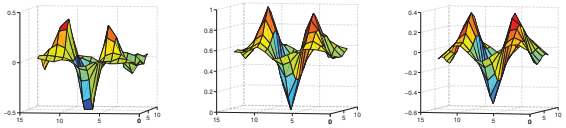

(a) true $\mathbf{h}$ (b) $\hat{\mathbf{h}}$(proposed) (c) $\hat{\mathbf{h}}$ ([4])

Fig. 2. Original and estimated PSFs.

Table 1. Performance of reflectivity image estimation.

Methods	ISNR$_{(dB)}$	NRMSE$_{(dB)}$	PSNR$_{(dB)}$
Proposed	8.7597	0.8018	18.5373
[4]	4.1089	1.3696	18.0123

Table 2. Performance of PSF estimation.

Methods	NRMSE$_{(dB)}$	PSNR$_{(dB)}$
Proposed	0.7392	9.2301
[4]	0.7805	8.7575

The results in Fig. 2 allow the performance of the PSF estimation to be appreciated. Figs. 2(c), 2(b) display the estimated PSFs obtained with the method of [4] and our approach. The interest of estimating the PSF jointly with the image is confirmed by the quantitative metrics provided in Table 2 comparing the true PSF with its estimates obtained with the proposed method and the method of [4].

[1] $\text{BSNR} = 10\log_{10}\frac{\|\mathbf{Hx}-\text{mean}(\mathbf{Hx})\|_2^2}{N\sigma_n^2}$

4. CONCLUSIONS

This paper proposed a hierarchical Bayesian model for the joint estimation of an ultrasound image and the system PSF. In order to solve this ill-posed problem, generalized Gaussian priors were assigned to the reflectivities of homogeneous regions of the image and a Gaussian prior was chosen for the PSF. The results obtained on simulated US data clearly highlight the interest of updating the PSF during the deconvolution process. Future work includes the application of our algorithm to real US data and the study of new estimation algorithms with reduced computational complexity.

5. ACKNOWLEDGMENT

This work was supported by the thematic trimester on image processing of the CIMI Labex, Toulouse, France, under grant ANR-11-LABX-0040-CIMI within the program ANR-11-IDEX-0002-02.

6. REFERENCES

[1] R. Jirik and T. Taxt, "Two dimensional blind Bayesian deconvolution of medical ultrasound images," *IEEE Trans. Ultrason. Ferroelectr. Freq. Control*, vol. 55, no. 10, pp. 2140–2153, 2008.

[2] J. Ng, R. Prager, N. Kingsbury, G. Treece, and A. Gee, "Wavelet restoration of medical pulse-echo ultrasound images in an EM framework," *IEEE Trans. Ultrason. Ferroelectr. Freq. Control*, vol. 54, no. 3, pp. 550–568, 2007.

[3] M. Alessandrini, S. Maggio, J. Poree, L. D. Marchi, N. Speciale, E. Franceschini, O. Bernard, and O. Basset, "A restoration framework for ultrasonic tissue characterization," *IEEE Trans. Ultrason. Ferroelectr. Freq. Control*, vol. 58, no. 11, pp. 2344–2360, 2011.

[4] N. Zhao, A. Basarab, D. Kouam, and J.-Y. Tournerets, "Restoration of ultrasound images using a hierarchical Bayesian model with a generalized Gaussian prior," in *Proc. IEEE Int. Conf. Image Process. (ICIP 2014), Paris, France*, 2014.

[5] O. Michailovich and D. Adam, "A novel approach to the 2-D blind deconvolution problem in medical ultrasound," *IEEE Trans. Med. Imag.*, vol. 24, pp. 86–104, 2005.

[6] J. A. Jensen and S. Leeman, "Nonparametric estimation of ultrasound pulses," *IEEE Trans. Biomed. Eng.*, vol. 41, no. 10, pp. 929–936, Oct. 1994.

[7] R. Morin, S. Bidon, A. Basarab, and D. Kouame, "Semi-blind deconvolution for resolution enhancement in ultrasound imaging," in *Proc. IEEE Int. Conf. on Image Process. (ICIP 2013), Melbourne, Australia*, 2013.

[8] L. Chaari, J.-C. Pesquet, J.-Y. Tourneret, P. Ciuciu, and A. Benazza-Benyahia, "A hierarchical Bayesian model for frame representation," *IEEE Trans. Signal Process.*, vol. 58, no. 11, pp. 5560–5571, 2010.

[9] W. K. Hastings, "Monte Carlo sampling methods using Markov chains and their applications," *Biometrika*, vol. 57, no. 1, pp. 97–109, 1970.